Hindawi
Journal of Chemistry
Volume 2022, Article ID 1196244, 11 pages
https://doi.org/10.1155/2022/1196244

Research Article

1,5-Dichloroethanoanthracene Derivatives As Antidepressant Maprotiline Analogs: Synthesis, DFT Computational Calculations, and Molecular Docking

Mujeeb A. Sultan,[1] **Renjith Raveendran Pillai**,[2] **Eman Alzahrani**,[3] **Ahmed A. Alsofi**,[1] **Sadam A. Al-Qadhi**,[1] **and Rami Adel Pashameah**[4]

[1]*Department of Pharmacy, Faculty of Medical Sciences, Aljanad University for Science and Technology, Taiz, Yemen*
[2]*Department of Physics, University College, Thiruvananthapuram, Kerala, India*
[3]*Department of Chemistry, College of Science, Taif University, P.O. Box 11099, Taif 21944, Saudi Arabia*
[4]*Department of Chemistry, Faculty of Applied Science, Umm Al-Qura University, Makkah 24230, Saudi Arabia*

Correspondence should be addressed to Mujeeb A. Sultan; mujeeb.aa@just.edu.ye

Received 4 June 2022; Revised 30 August 2022; Accepted 2 September 2022; Published 23 September 2022

Academic Editor: Wagdy Eldehna

The chlorinated tetracyclic 1,5-dichloro-9,10-dihydro-9,10-ethanoanthracen-12-yl)-N-methylmethanamine **1**, a maprotiline analog, has been synthesized via reduction and the Diels–Alder reaction followed by reductive amination of aldehyde **2**.1D-NMR (DEPT) and 2D-NMR (HSQC, DQF-COSY) techniques were recruited for structural elucidation in addition to HRMS. Density functional theory calculations were performed to identify the possible isomers of the intermediate compound aldehyde **2**; these calculations were in good agreement with experimental results where aldehyde **2** could exist in three isomers with comparable energies. In addition, the side chain of this aldehyde **2** was extended via the Wittig reaction to obtain the unsaturated ester **5** that was subjected to selective olefinic catalytic hydrogenation to obtain the corresponding saturated ester **6**. Molecular docking simulation showed that all the compounds (**1**, **2**, **5,** and **6)** have high antidepressant activities and form stable complexes with LeuT by inhibiting the neurotransmitter reuptake at the synapse and hence are good candidates as antidepressant drugs.

1. Introduction

Anthracenes are simply and efficiently incorporated into several organic reactions and are proved to have a wide range of industrial applications such as in fluorescent sensors [1, 2], laser dyes [3], and supramolecular assemblies [4, 5]. Their application in pharmaceutical agents is another interesting field.

From the organic synthesis point of view, 1,5-dichloroanthracene was functionalized through the Kumada coupling to access a series of 1,5- functionalized anthracenes [6]. Based on 1,5-dichloroanthracene, many macrocyclic compounds have been synthesized and reported in the literature [7–9]. 1,5-dichloroanthracene was allowed to react with 3-chlorobenzene through the Diels–Alder (DA) reaction to access substituted triptycene derivatives [10, 11]. Starting from 1,5-dichloroanthracene and other anthracenes, a series of SiMe3-functionalized anthracene derivatives were synthesized via multistep cross-coupling reactions and NMR-qualitatively studied towards UV irradiation [12].

From a biological point of view, 1,5-dichloroanthracene itself shows antioxidant activities through proton transfer mechanisms [13]. A variety of 1,5-dichloroanthracene- and anthraquinone-related derivatives proved to possess an anti-inflammatory activity with no significant cytotoxicity in human neutrophils [14] and other anthracene analogs displayed potent anti-inflammatory activity against superoxide anion production and induced apoptosis, thus exerting antitumor activity [15].

1,5-dichloroethanoanthracene derivatives are related in structure to the antidepressant drug maprotiline 9,10-dihydro-N-methyl-9,10-ethanoanthracene-9-propanamine

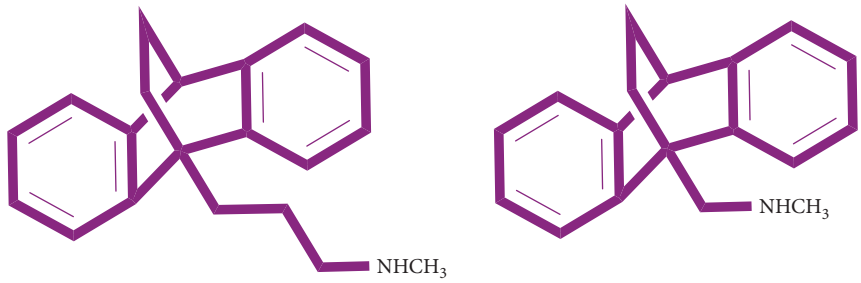

Maprotiline Benzoctamine

Figure 1: Structures of the ethanoanthracene pharmaceutical agents: maprotiline and benzoctamine.

(Figure 1), which exhibits *in vitro* antiproliferative activity against Burkitts's Lymphoma (BL) cell lines DG-75 [16] and induce anti-multidrug resistance (MDR) effect in the cancer cell lines, and plasmodium falciparum [17] as well the derivatives of 1,5-dichloroethanoanthracene are related in structure to benzoctamine 9,10-dihydro-9-(methylaminomethyl)-9,10-ethanoanthracene (Figure 1) that have been used to treat anxiety and tension [18]. Ethanoanthracene derivatives were described as therapeutically effective agents for treating neurodegenerative disorders and neurotoxic injury [19]. Another similar class of 9,10-dihydro- 9,10-ethanoanthracenes has been reported [20–22].

The serotonin transporter (SERT) has been considered to be the primary target for the treatment of major depressive and anxiety disorders [23, 24]. The most widely used antidepressants for the treatment of major depressive disorders are selective serotonin reuptake inhibitors, which inhibit serotonin uptake from the synaptic space into presynaptic neurons [25, 26]. It has been shown that serotonin reuptake inhibitors have contrasting chemical structures, which resulted in compounds with considerable pharmacological activities.

Designing and synthesizing new 1,5-dichloroethanoanthracene derivatives is not straightforward and is considered as imperative challenges that more than one isomer will be obtained in the first step of 1,5-dichloroanthracene functionalization. However, we were delighted to synthesize 1,5-dichloroethanoanthracenes (**1**, **2**, **5,** and 6) and discover their structures by using different spectroscopy techniques including 2D-NMR. In addition, computational calculations were performed in order to identify the possible isomers of the aldehyde 1,5-dichloroethanoanthracene **2**. Moreover, in the present study, molecular docking simulation was employed to investigate the binding mechanism of the compounds (**1**, **2**, **5,** and **6)** in the active binding site of a bacterial leucine transporter (LeuT) using the high-resolution structure of SERT (PDB : 2QJU) [27]. These compounds and standard antidepressant maprotiline were docked into the central active site of the SERT protein.

2. Results and Discussion

*2.1. Retrosynthetic Analysis and Strategy for Chlorinated Maprotiline Analog **1**.* We began the synthesis with the intention of obtaining the products efficiently in high yields, lowering the number of steps, high level of selectivity, high level of atom economy, making it environmentally friendly, and at a low cost. The retrosynthetic breakdown of our target chlorinated maprotiline analog **1** yields two fragments; the tetracyclic intermediate with its bridged dihydroethanoanthracene system **I** and anthracene precursor **3** (Scheme 1). The target compound **1** could be obtained by functional group interconversion (FGI) of the key intermediate **2**. The key intermediate **2** with its system [2.2.2] could be built in one step via a DA reaction between a suitable dienophile possessing a functional group and the 1,5-dichloroanthracene **3** center ring as a diene. Acrolein is a reactive dienophile in the DielsF02DAlder reaction and its reaction with 1,5-dichloroanthracene **3** could lead to the aldehyde functionality, which allows us to access other functional groups via FGI including the target amine **1**. Precursor **3** can be prepared from a commercially available 1,5-dichloroanthraquinone **4**, as described in the literature [6].

*2.2. Synthesis of the Chlorinated Maprotiline Analog **1**.* The target compound **1** was obtained according to the synthetic pathway (Scheme 2). The intermediate 1,5-dichloro-9,10-dihydro-9,10-ethanoanthracene-12-carbaldehyde **2** was prepared by HCl-catalyzed reduction of 1,5-dichloroanthraquinone **4** followed by DA reaction of 1,5-dichloroanthracene **3** with acrolein. In fact, it attempts to react 1,5-dichloroanthracene **3** with acrolein to yield aldehyde **2** under a variety of conditions which were not successful. TLC monitoring of these attempts reactions showed that a substantial amount of starting materials remained unreacted; this may refer to the presence of chlorine atoms on anthracene that render it a poor electron-donating diene. Then, 1,5-dichloroanthracene **3** was allowed to react with acrolein using boron trifluoride etherate ($BF_3{\cdot}OEt_2$) as a catalyst, at room temperature as well at F02D15F06F Celsius to yield compound **2** but as three isomers in a ratio of 1 : 1:1.75 were deduced from the ^{1}H-NMR spectrum (Figure. S1). The IR spectrum supported the structure of compound **2** and showed stretching vibration of the carbonyl group (CHO) as a strong peak at 1723 cm^{-1} (Figure. S2). Theoretically, compound **2** could exist in more than one isomer and conformer form, due to its three stereocenters as well due to the possible different spatial positions of the CHO group in relation to benzene

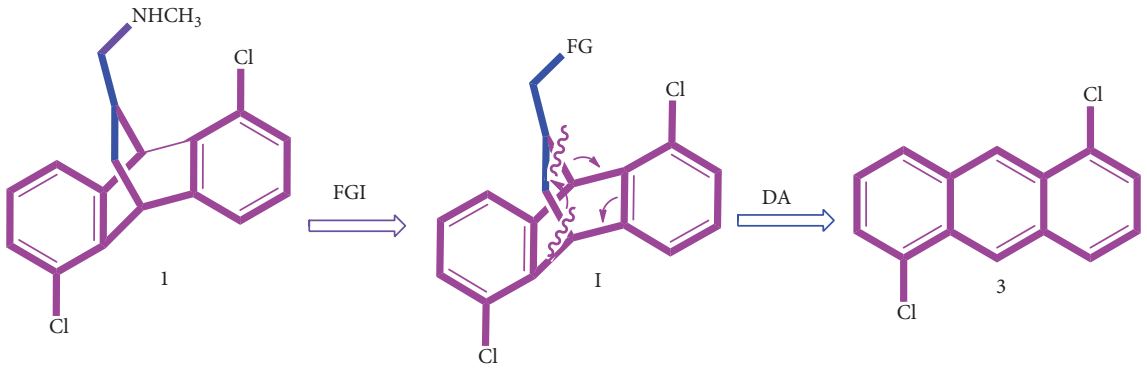

Scheme 1: The retrosynthetic analysis and strategy for compound **1**.

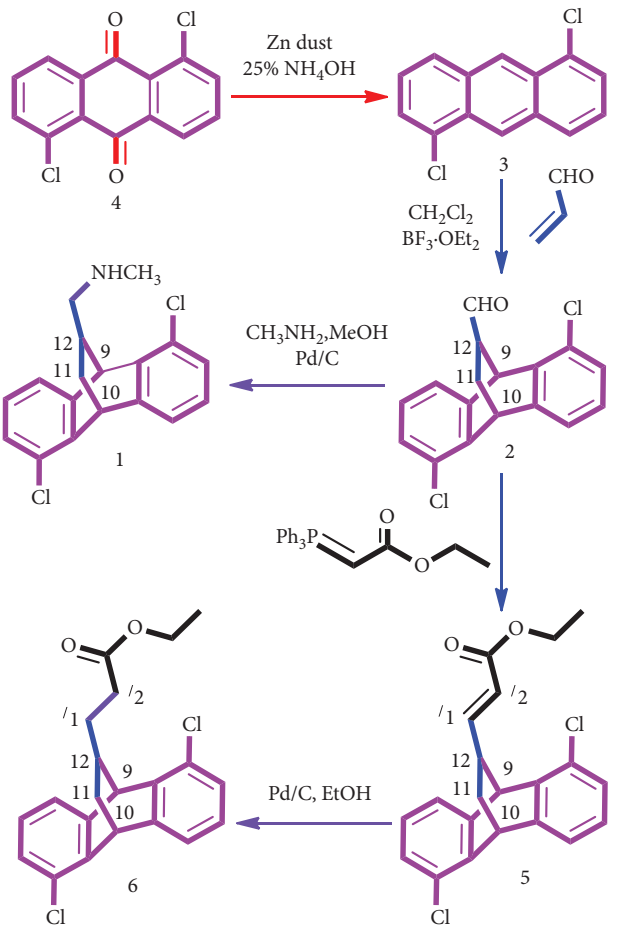

Scheme 2: Synthesis of 1,5-dichloroethanoanthracene derivatives.

rings; in contrast, the C2 symmetry of the reactant 1,5-dichloroanthracene **3** could reduce the number of the product isomers. Computational calculations were in the same line, where three conformers were identified as presented in Table 1 and Figure 2. Different solvent systems were recruited to purify these isomers, among which the hexane: toluene (1 : 1) mixture was the best one. Unfortunately, the three isomers of aldehyde **2** could not be separated individually, so we have no chiral columns.

Table 1: DEPT and HSQC results of the target amine **1**.

Carbon NO.	*Chemical shift δ*			
	^{1}H (M, *J*)	^{13}C		
		δ	DEPT 90	DEPT 135
CH_3	2.32 (s)	33.39		(↑CH_3)
C1′, CH_2	2.25–2.29 (m), 2.43–2.47 (m)	54.31		(↓CH_2)
C9	4.47 (d, 1.64)	46.05	(↑CH)	(↑CH)
C10	4.29 (t, 2.12)	43.73	(↑CH)	(↑CH)
C11, CH_2	1.25–1.28 (m), 1.95–2.11 (m)	33.02		(↓CH_2)
C12	2.25–2.29 (m)	35.80	(↑CH)	(↑CH)

However, after several trials of normal column chromatography, the two isomers (called 2a) were initially eluted together (Figure S3(a) and Figure S4) while the third isomer (called 2b) was purely separated alone (Fig. S3(b), Figure S5, and Figure S6). The protons of the CHO group of the aldehyde 2a appeared separately as doublet signals at *δ* 952 and 9.56 ppm with coupling constant *J* 0.8 Hz for each, whereas the signals of bridgehead protons appeared collectively; and the signal of the protons integrated for carbon 10 (C10) appeared as pentet at *δ* 4.93 ppm with coupling constant $J = 2.74$ Hz and the signal of the protons integrated for carbon 9 (C9) appeared as a double doublet at *δ* 5.26 ppm with coupling constant $J = 7.2$ and 2.45 Hz (Figure. S3(c)).

The ^{1}H and ^{13}C spectra of the isomer **2b** can be divided into two regions: aromatic and aliphatic (Figure. S5, Figure. S6). In the aromatic region, multiple regions at *δ* 7.21–7.45 ppm were assigned for the protons integrated for anthracene rings and this region is exhibited in the ^{13}C spectrum as peaks at *δ* 123.45–144.06 ppm. In the aliphatic portion, there is a triplet signal at *δ* 4.44 ppm with a coupling constant *J* 0.8 Hz assigned for the protons integrated for carbon 10 (C10) and a doublet signal *δ* 4.72 ppm with a coupling constant *J* 0.8 Hz assigned for the protons integrated for carbon 9 (C9). These signals correspond to the peaks that appeared at *δ* 43.69 and 45.20 ppm in the ^{13}C spectrum, respectively; these signals are considered as one of the two markers indicating DA cycloaddition adduct **2b** (Figure. S5(b)). The multiplet signals that appeared at *δ* 1.99–2.06 and 2.11–2.18 ppm are assigned to the protons of

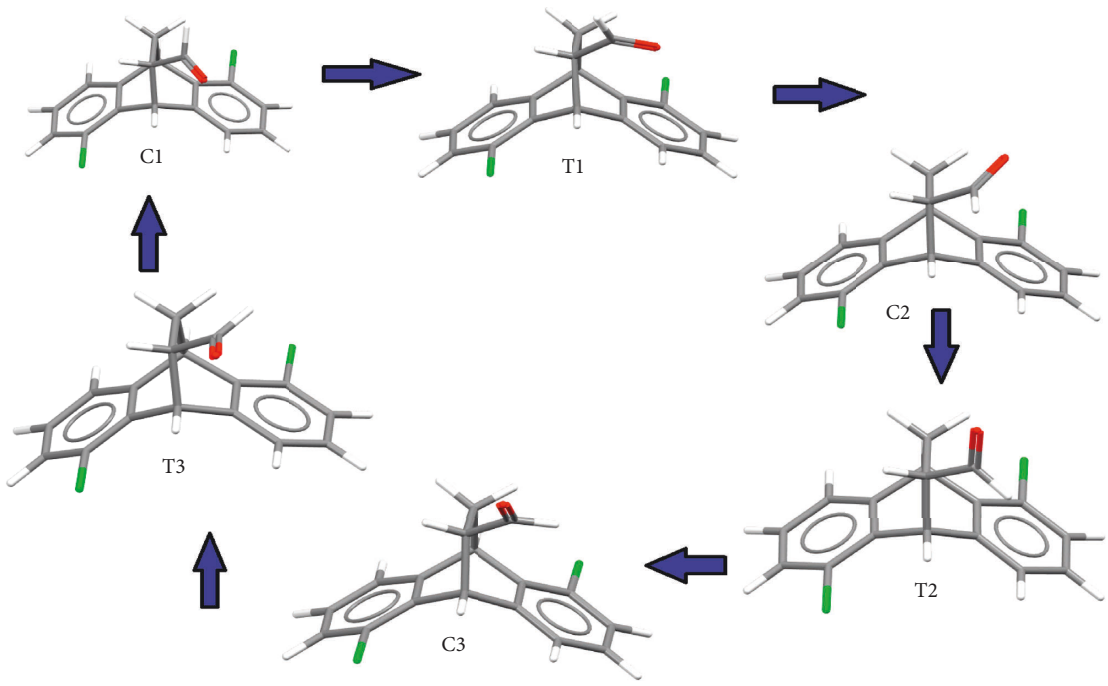

Figure 2: Conformational interconversion of the various minimum (C) and transition state (T) conformers of compound **2**.

carbon 11 (C11) that appeared at δ 28.76 ppm in the ^{13}C spectrum and the ^{1}H multiplet signal that appeared δ 2.77–2.84 ppm is assigned to the proton of carbon 12 (C12) that appeared at δ 51.22 ppm in ^{13}C spectrum. The aldehyde signal is considered as the second marker indicating DA cycloaddition adduct **2b,** and this signal represents the only aldehyde proton in the expected structure **2b** and appears as a doublet at δ 9.45 ppm with a coupling constant $J = 0.8$ Hz as well as ^{13}C NMR confirms the existence of aldehyde group (CHO) as a single peak at δ 202.73 ppm.

Reductive amination of the aldehyde **2** was achieved by using a combination of a commercially available solution of methylamine in methanol, molecular hydrogen, and Pd–C produced target amine 1. Generally, the two commonly used reductive amination protocols are based on either catalytic hydrogenation or hydride reducing agents; in contrast to hydride reducing agents, the use of molecular hydrogen is economically attractive [28–33]. The ^{1}H and ^{13}C NMR analysis of the target amine 1 is similar to its precursor 2 with slight differences but the signal of CHO disappeared in amine 1 and IR supported this finding (Figure 3), in addition to the appearance of singlet signal at δ 2.32 ppm that assigned to the methyl protons (-N-CH3) and correspond to the peak at δ 33.39 ppm in the ^{13}C NMR spectrum. For further structural elucidation of the target compound **1**, distortionless enhancement by polarization transfer (DEPT) and heteronuclear single quantum coherence spectroscopy (HSQC) were run and are presented in Table 2 and Figure S8, Figure S9, and Figure S10. It is well known that only CH groups appear as positive signals (↑CH) in the DEPT-90 spectrum, whereas in the DEPT-135 spectrum, CH_3 and CH groups appeared as positive signals (↑CH, ↑CH_3) but CH_2 groups appeared as negative signals (↓CH_2). The DEPT-90 spectrum of amine **1** shows three positive signals (↑CH) at δ 35.80, 43.73, and 46.05 ppm assigned to C12, C10, and C9, respectively (Figure. S8). The DEPT-135 spectrum shows four positive signals and two negative signals; among them, three positive signals were assigned to the three CH groups and the fourth positive one was assigned to the carbon of methyl group (CH_3) that appeared at δ 33.39 ppm, the two negative signals that appeared at δ 33.02 and 54.31 ppm were assigned to methylene groups (–CH_2–) of C11 and C1, respectively (Figure. S9).

HSQC experiments permit to obtain high-quality spectra of the protons attached to a specific carbon. According to the HSQC spectrum (Figure. S10), the structure of amine **1** is clearly elucidated and the H atoms that are attached to the carbon atoms are shown in Table 1. Interestingly, the two protons assigned to C11 have appeared in separate regions; one of them appeared at δ 1.25–1.28 ppm as multiple signals; although, it appeared as an overlapped triplet signal when enlarging this spectra region, and the other proton appeared at δ 1.95–2.11 ppm as multiple signals.

*2.3. Extending the Side Chain of the Aldehyde **2** via the Wittig Reaction.* Aldehyde **2** was subjected to a Wittig olefination reaction employing two equivalents of the air-stable stabilized commercially available Wittig reagent (carbethoxymethylene) triphenylphosphorane (Scheme 2). The reaction was smoothly run at room temperature in dichloromethane (CH_2Cl_2) to give α,β-unsaturated ester 5 in 76% yield as a mixture of cis and trans isomers. The NMR J-coupling and chemical shift of the vinylic protons were recruited to differentiate between the cis and trans isomers. Based on the integration of the vinylic proton signals, the ratio of the cis and trans was approximately 1 : 3.5 (Figure. S11(a)–S11(c)). The ^{1}H-NMR spectrum of the trans isomer exhibited a

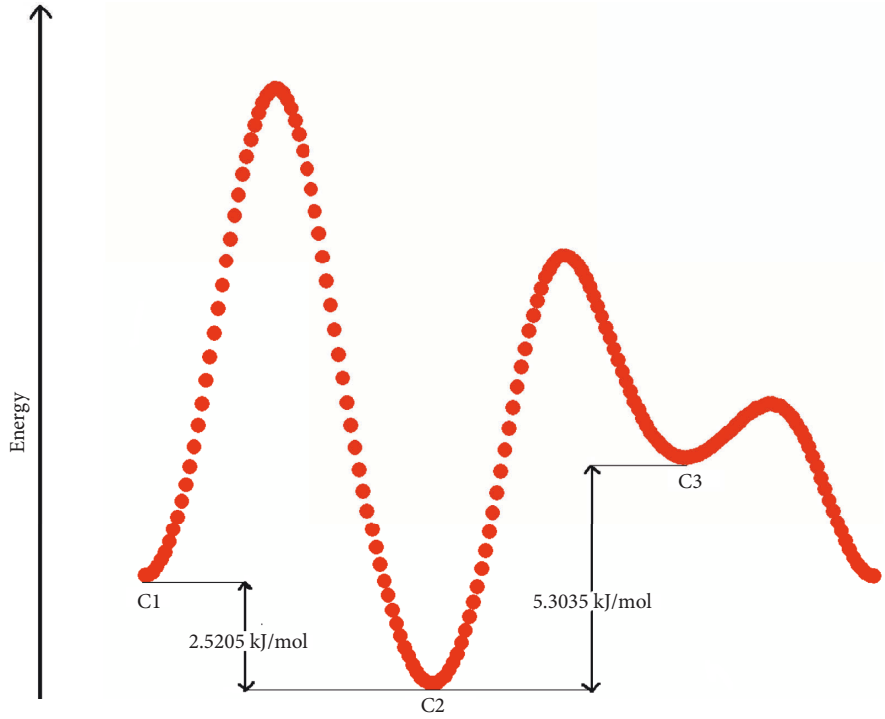

Figure 3: Binding modes of (a) the native ligand, desipramine, (b) standard drug, maprotiline, (c) compound 1, (d) compound **2**, (e) compound **5,** and (f) compound **6** and at the central binding site of LeuT.

Table 2: Energies (a.u.) of the predicted conformations of the compound **2**.

Parameter	2-C1	2-C2	2-C3
E_{Tot}	−1650.88155	−1650.88251	−1650.88049

doublet signal at δ 5.78 ppm with coupling constants $J = 25$ Hz assigned for olefinic proton attached to C′2 (-C=**CH**–COOEt) and a double doublet signal at δ 6.45 ppm with coupling constant $J = 15$, 5 Hz assigned for an olefinic proton attached to C′1 (-**CH**=C-) (Figure. S11(b)). The IR spectrum of the unsaturated ester **5** displayed characteristic absorption of the enone system at υ 1650 cm^{-1} (C=C) together with the absorption peak of (C=O) at υ 1709 cm^{-} 1(Figure. S12). For further structural elucidation of compound **5**, HSQC were run and are presented in Figure. S13. α,β-unsaturated ester **5,** product of the Wittig reaction, was then subjected to selective hydrogenation to reduce (C=C) double bond using palladium on carbon (Pd/C) as catalyst under H_2 in ethanol at room temperature to obtain the saturated ester **6** in a yield of 42%. The NMR spectra of saturated ester **6** were clear where the signals of olefinic protons of the precursor **5** disappeared and instead, the triplet signal appeared at δ 2.33 ppm with coupling constant $J = 12$ Hz assigned for the protons attached to the C′2 (-C$\mathbf{H_2}$-COOEt) (Figure. S14). For further structural elucidation of saturated ester **6,** homonuclear correlation ^{1}H–^{1}H correlation, a double-quantum filtered correlation spectroscopy (DQF-COSY) technique was employed to assign proton chemical shifts (Figure. S15). HSQC experiments were performed to determine the protons attached to a specific carbon (Figure. S16) and high-resolution mass spectroscopy (HRMS) was used to specify the molecular weight (Figure. S17)**.** The NMR-based structural elucidations of these compounds were clear and valuable; however, the correlation study between experimental and theoretical NMR values will be more valuable than what is reported in the literature [34, 35].

2.4. DFT; Conformer Analysis. Conformational analysis of compound **2** revealed three minima and three transition states (Figure 2). The absence of imaginary frequencies on the calculated vibrational spectrum confirms the global minimum energy for all the conformers. Different conformers of compound **2** were found by carrying out a potential energy scan on the C–C bond connecting the aldehyde group (CHO) with the fused ring structure. The relative energies (kJ/mol) of different conformations are tabulated and are displayed in Table 2. The **2-C2** conformer was found to be the most stable, which is lower in energy than the other two conformers **2-C1** and **2-C3** by 2.5205 kJ/mol and 5.3035 kJ/mol, respectively (Figure 4).

The low energy of the **2-C2** conformer may be the result of the electrostatic interaction between the electropositive region or σ hole of the chlorine atom, which serves as a Lewis acid, and the carbonyl oxygen, which serves as a Lewis base (Figure 4) and is analogous to a classical hydrogen bonding. This result is supported by the most "provisional recommendation" by IUPAC [36], which states that there is an interaction between the nucleophilic region of carbonyl oxygen and the electrophilic region of a halogen atom. More DFT confirmation and analysis of energy plane using TD-

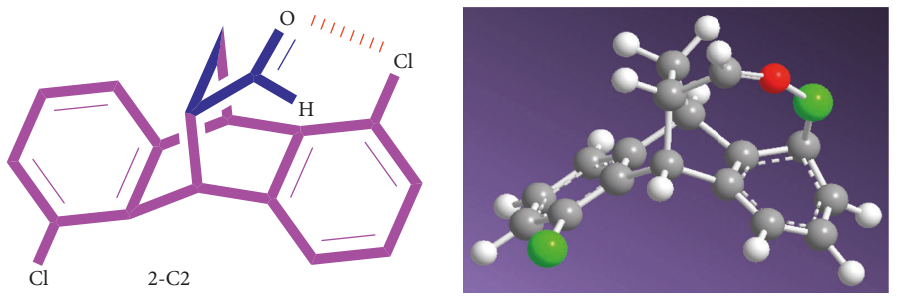

Figure 4: Plausible intramolecular interaction between chlorine (Cl) and oxygen (O) in **2-C2.**

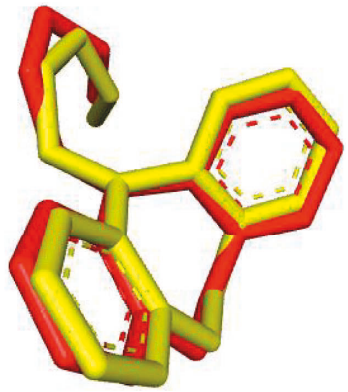

Figure 5: The docked pose (yellow) and the crystal structure conformation (red) of desipramine, the native ligand.

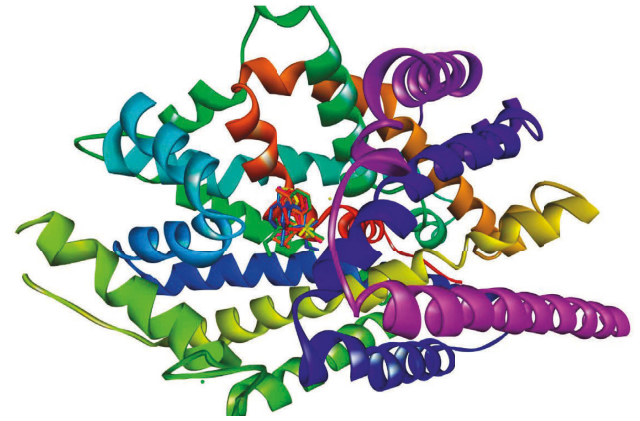

Figure 6: The docked structures of the co-crystallized ligand, desipramine (red), and standard drug maprotiline (yellow) along with the compounds **1** (orange), **2** (pink), **5** (green), and **6** (blue) in the binding site of LeuT.

DFT and UV-visible to know more about the conformer's differences are recommended [37, 38].

2.5. Molecular Docking. In order to verify the docking protocol, we have removed the co-crystallized ligand, desipramine, from the crystallized structure of LeuT and then redocked it at the same binding site. The root mean square deviation (RMSD) between the docked pose and the crystal structure conformation of desipramine was found to be less than 1 Å (Figure 5), which indicates the quality of the docking procedure [39]. All the compounds (**1**, **2**, **5,** and **6**) and the standard drug, maprotiline, were prepared for docking by minimizing their energies using the density function theory (DFT) at the B3LYP/6-311G(d, p) level of theory.

Among fifty docked confirmations obtained, one which has the lowest binding energies (−7.34 kcal/mol for compound **1**, −6.60 kcal/mol for compound **2**, −6.62 kcal/mol for compound **5**, −6.94 kcal/mol for compound **6** and 7.93 kcal/mol for the standard drug maprotiline) was selected for analyzing binding interactions within the active site of LeuT using Discovery Discover Studio Visualizer4.0 software [40] and Chimera [41]. The docked structure of the standard drug maprotiline, co-crystallized ligand, desipramine, and synthesized compounds (**1**, **2**, **5** and **6**) with LeuT crystal structure is shown in Figure 6. The binding poses and the interactions corresponding to the lowest energy conformations of the compounds at the central binding site of the LeuT protein are shown in Figure 7.

From Figures 7 and 8, it is clear that the amino acid residues responsible for the binding mechanism of all the derivatives in the active site are Arg30, Val33, Ile111, Ala319, and Phe320. As in the same manner by which the native ligand, desipramine and standard drug, maprotiline has the hydrogen bond interaction with Asp401, the amino group of compound **1** also forms a hydrogen bond with amino acid residue Asp401 in the binding site with a bond length of 1.97 Å. In the case of compounds **2**, **5,** and **6**, there are no observable hydrogen bonds with the amino acid residue ASP401. From the analysis of the binding mechanism, it is clear that all compounds **1**, **2**, **5**, and **6** show hydrophobic interactions with amino acid residues Arg30, Val33, Ile111, Ala319, and Phe320. The binding energy values and binding interactions show that all the compounds form stable complexes with the SERT protein by interacting with the important amino acids present in the central binding site similar to the native ligand, desipramine and the standard drug, maprotiline.

3. Experimental Methods

3.1. Chemistry Protocols. Most of the reagents and solvents were of analytical grade. Starting chemicals were purchased from Aldrich (Merck). A Perkin Elmer 240 elemental

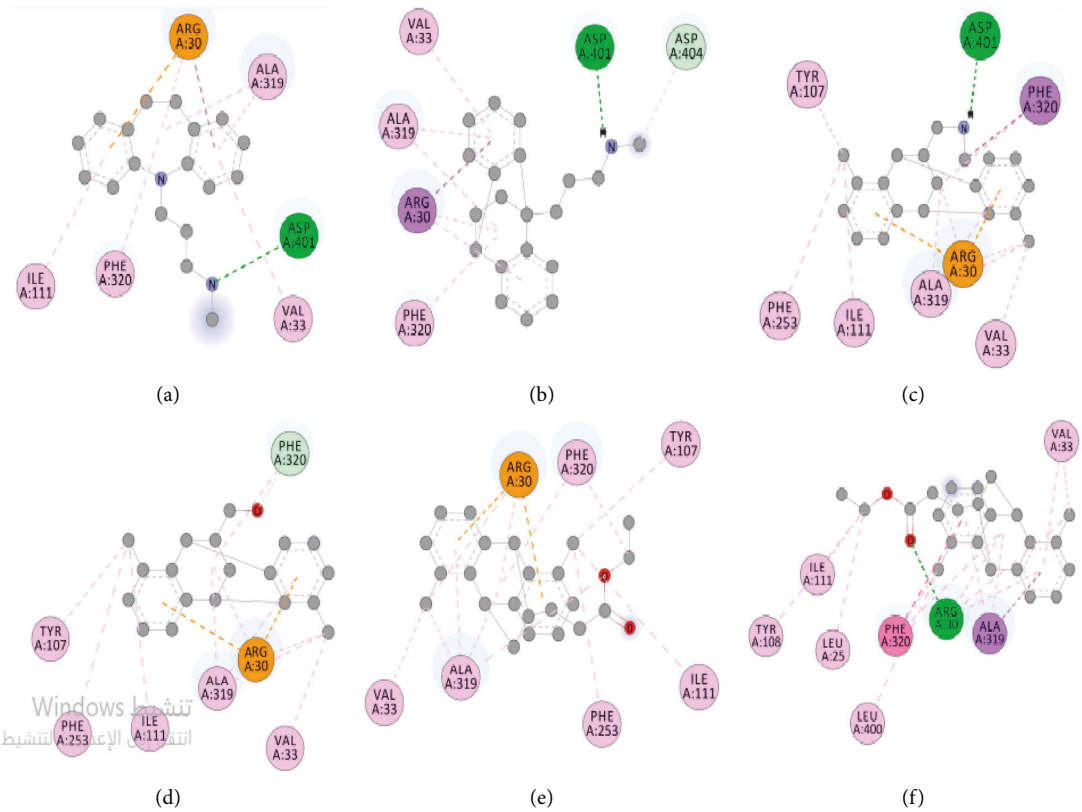

FIGURE 7: Potential energy scan profiles for the conformational interconversion of the conformers **2-C1**, **2-C2,** and **2-C3**.

analyzer was used to obtain the infrared (IR) spectrum. ^{1}H and ^{13}C-NMR spectra were recorded on either Joel 400 MHz or Bruker 500 MHz. Mass spectra (MS) and high-resolution mass spectra (HRMS) data were obtained on a Q-Tof Premier UPLC-MS. Reactions were monitored using thin-layer chromatography (TLC) plates (Merck, Germany), stained with valine and then spots were detected with a 254 nm UV lamp. Silica gel (35–70 mesh) was employed in column chromatography purification.

3.2. Synthesis

3.2.1. Synthesis of 1,5-Dichloroanthracene ***3*** *[6, 42].* 1,5-Dichloroanthraquinone **4** (10.0 g, 36.1 mmol) and zinc dust (50.0 g, 765 mmol) were suspended in 200 mL of aqueous 28% NH_3 with stirring for 3 h at 100 degree Celsius. After cooling to r.t., the reaction mixture was separated by filtration and the filtrate was eluted and extracted several times with CH_2Cl_2. The CH_2Cl_2 organic phases were collected, dried over $MgSO_4$, filtered, and concentrated under a vacuum. To the residual crude, 500 mL isopropanol and 50 mL aqueous HC1 (12 M) were added. After refluxing the reaction mixture for 3 h, the mixture was cooled, concentrated in vacuo and then partitioned between CH_2Cl_2 and aqueous 5% $NaHC0_3$. The CH_2Cl_2 organic phase was collected, dried with $MgSO_4$, filtered, and concentrated to give crude 1,5-dichloroanthracene **3**. This crude was crystallized using a CH_2Cl_2-petroleum ether mixture. The product 1,5-dichloroanthracene **3** was dried in the air for 24 h (7.5 g, 30.49 mmol) as yellow-orange needles in a 84.45% yield; mp 187–188 Celsius degree; IR (KBr): υ = 681, 720, 736, 778, 849, 873, 903, 958, 996, 1145, 1162, 1212, 1300, 1449, 1530, and 1618 cm^{-1}; ^{1}H-NMR ($CDCl_3$, 400 MHz): δ = 7.40–7.61 (m, 4 H, ArH), 8.00 (dd; J = 2.92 Hz, 2 H, ArH), 8.42 (s, 1 H, ArH), 8.84 (s, 1 H, ArH) ppm. ^{13}C NMR (CDCl3, 100 MHz): δ = 124.37, 125.42, 125.58, 126.29, 128.24, 131.7, 132.8 ppm.

3.2.2. Synthesis of 1,5-Dichloro-9,10-dihydro-9,10-ethanoanthracene-12-carbaldehyde ***2.*** Into a previously F02D15 Celsius degree cooled solution of 1,8-dichlorolanthracene **3** (500 mg, 2 mmol) in 70 mL CH_2Cl_2, acrolein (0.65 mL, 9.3 mmol) was added. Then, BF3·OEt2 (0.5 mL, 4.05 mmol) was added dropwise and the mixture was allowed to stir at -15 Celsius degree for 1 hour then at room temperature for 4 hours. The reaction was then quenched with sat. NaCl and extracted with CH_2Cl_2. The organic layers were collected, dried with Na_2SO_4, filtered and concentrated. The crude product was preliminary purified by column chromatography on silica gel using dichloromethane-petroleum ether (1 : 1) to obtain aldehyde **3** (450 mg, 1.49 mmol) as three isomeric adducts in a 74% yield; IR (KBr): υ = 576, 706, 775, 1169, 1264, 1458, 1570, 1723, 2961, 3024,and 3047 cm^{-1}. A mixture of isomeric adducts (300 mg, 1 mmol) was separated by column chromatography on silica gel (1:1-hexane:toluene) to give the initially eluted two isomers of **2 (2a)** (160 mg, 0.53 mmol) as yellow viscous with the following

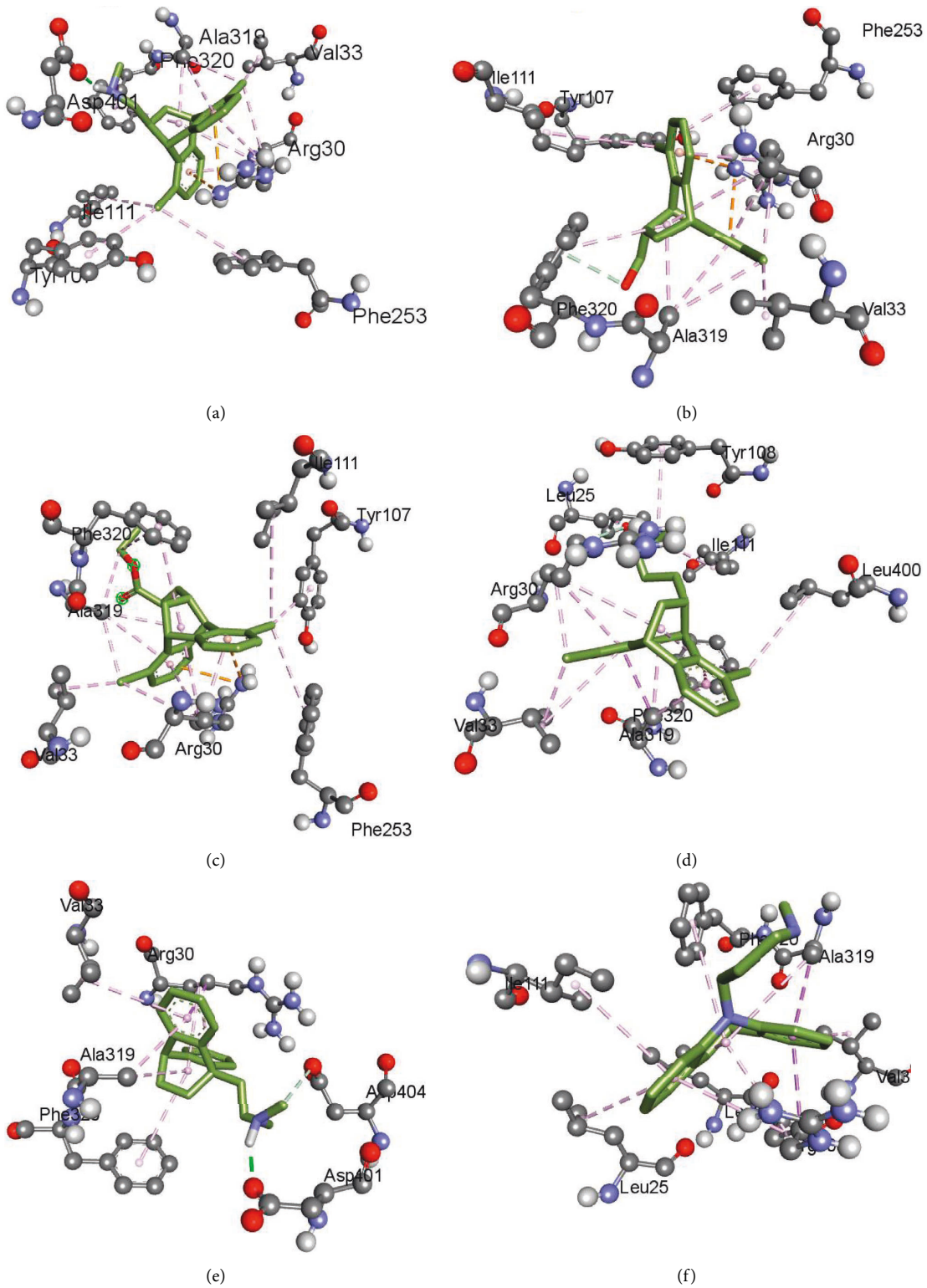

FIGURE 8: Binding modes of (a) compound **1**, (b) compound **2**, (c) compound **5,** (d) compound **6**, (e) standard drug maprotiline, and (f) the native ligand, desipramine at the central binding site of Leu T.

characteristics: ^{1}H-NMR ($CDCl_3$, 400 MHz): $\delta = 1.93$–2.04 (m, 2H, H–C11), 2.14–2.22 (m, 2H, H–C11), 2.8–2.89 (m, 2H, H–C12), 4.93 (pent, $J = 2.74$ Hz, 2H H–C10), 5.26 (dd, $J = 7.2$, 2.45 Hz, 2H, H–C9), 7.1–7.47 (m, 12H, H–Ar), 9.52 (d, $J = 0.8$, ^{1}H, H–CHO), and 9.56 (d, $J = 0.8$, ^{1}H–CHO) ppm. ^{13}C NMR (CDCl3, 100 MHz): $\delta = 27.29$, 27.32, 40.37, 41.50, 41.59, 49.87, 51.07, 122.45, 122.48, 122.56, 123.54, 123.77, 126.78, 127.11, 127.17, 127.24, 127.28, 127.50, 127.78, 129.35,

123.38, 129.57, 130.23, 136.58, 138.98, 140.61, 140.79, 140.94, 143.25, 145.08, 145.37, 200.91, 201.17 ppm, and a pure isomer of **2** (**2b)** (140 mg, 0.46 mmol) as a white solid with the following characteristics: ^{1}H-NMR ($CDCl_3$, 400 MHz): δ = 1.99–2.06 (m, ^{1}H, H–C11), 2.11–2.18 (m, ^{1}H, H–C11), 2.77–2.84 (m, ^{1}H, H–C12), 4.44 (t, J = 0.8 Hz, 1H, H–C10), 4.72 (d, J = 0.8 Hz, ^{1}H, H–C9), 7.21–7.45 (m, 6H, H–Ar), and 9.45 (d, J = 0.8, ^{1}H, H–CHO) ppm. ^{13}C NMR (CDCl3, 100 MHz): δ = 28.76, 43.69, 45.20, 51.22, 123.45, 123.51, 123.64, 124.53, 125.96, 125.99, 126.28, 126.55, 139.37, 142.12, 143.79, 144.06, and 202.73 ppm.

*3.2.3. Synthesis of 1,5-Dichloro-9,10-dihydro-9,10-ethanoanthracen-12-yl)-N-methylmethanamine **1** [43].* To a 5° mL two-neck round-bottom flask connected to a condenser capped with a H_2 balloon and a rubber septum, a 100 mg Pd–C catalyst was added. The flask was evacuated and backfilled with H_2 two times. Then, a solution of aldehyde **2** (50 mg, 0.165 mmol) in methanol (3 mL) and (0.25 mL, 2 M) methylamine solution in methanol were added to the flask by syringe through a septum. After 1.5 h of the reaction time, the reaction mixture was filtered and washed with CH_2Cl_2,,and the solvent was then removed to obtain amine **1** with the following characteristics: **IR (KBr):** υ = 706, 740, 1266, 1422, 2987, 3055 cm^{-1}, **^{1}H-NMR ($CDCl_3$, 500 MHz):** $\boldsymbol{\delta}$ = 1.25–1.28 (m, ^{1}H, H–C11), 1.95–2.11 (m, ^{1}H, H–C11), 2.25–2.29 (m, 2H, H–C12, H–C1$'$, CH_2), 2.32 (s, 3H, H–CH_3), 2.43–2.47 (m, ^{1}H, H–C1$'$, CH_2), 4.29 (t, J = 2.12, ^{1}H, H–C10), 4.47 (d, J = 1.64, ^{1}H, H–C9), 7.07–7.17 (m, 3H, ArH), and 7.19–7.46 (m, 3H, ArH) ppm; **DEPT 90:** 35.80 (↑CH), 43.73 (CH), and 46.05 (↑CH); **DEPT 135:** 33.02 (↓CH_2), 33.39 (↑CH_3), 35.80 (↑CH), 43.73 (↑CH), 46.05 (↑CH), and 54.31 (↓CH_2) ppm; **MS (ES) *m/z* (%)** = 318 (100) [M$^+$], 284 (70), 250 (18), 184 (40), 117 (62), and 85 (40); **HRMS (ES)** Calcd for $C_{18}H_{18}$ NCl_2 [M$^+$] 318.0816, Found 318.0815.

*3.2.4. Synthesis of Z/E-Ethyl 3-(1,5-dichloro-9,10-dihydro-9,10-ethanoanthracen-12-yl)-propenoate **5**.* Into a 50-mL round-bottomed flask containing aldehyde **2** (755 mg, 2.5 mmol) predissolved in a 15 mL dichloromethane, a two equivalent Wittig reagent (carbethoxymethylene) triphenylphosphorane (174 mg, 5 mmol) was added. The reaction mixture was stirred overnight at room temperature; then, the solvent was removed to purify via silica gel column chromatography using the eluent system (ethyl acetate/petroleum ether, 1 : 20) obtaining unsaturated ester **5** as Z/*E* isomer (700 mg, 1.9 mmol, 76%) in ratio of 1 : 3.5, respectively, as a yellow oil with the following characteristics; **IR (KBr):** υ = 650, 735, 909, 1036, 1097, 1170, 1240, 1271, 1305, 1369, 1461, 1650, 1709, 2254, 2875, 2971, and 3537 cm^{-1}; **^{1}H-NMR ($CDCl_3$, 400 MHz): $\boldsymbol{\delta}$ =** 1.15–1.35 (m, 6H, H–CH_3 (*Z*/*E*)), 1.45–1.52 (m, ^{1}H, H-11), 2.07–2.12 (m, ^{1}H, H-11), 2.73–2.80 (m, ^{1}H, H-12), 4.12–4.18 (q, J = 25, 2H), 4.22 (d, J = 5, 1H, H-9), 4.26 (q, J = 25, 2H), 4.34 (t, J = 3, ^{1}H, H-10), 4.35 (t, J = 2, ^{1}H, H-10), 5.78 (d, J = 25 Hz, ^{1}H), 6.45 (dd, J = 15, 5, ^{1}H), 7.1–7.19 (m, 6H, ArH), and 7.25–7.35 (m, 6H, ArH) ppm. For only (*E*) **HSQC** and **^{13}C NMR ($CDCl_3$, 100 MHz): $\boldsymbol{\delta}$ =** 14, 33.9 (CH_3), 43 (CH_2, C11), 40.09 (C12), 43 (C10), 48 (C9), 59.8 (-O–CH_2–), 120.7, 122.9, 123.2, 123.5, 125.03, 125.06, 125.08, 125.1, 134, 139.5, 143.4, 143.6, 143.9, 152, and 167 ppm; **HRMS (ES)** Calcd for $C_{21}H_{18}$ O_2Cl_2Na [*M*+] 395.0582, Found 395.0576.

*3.2.5. Synthesis of Ethyl 3-(1,5-dichloro-9,10-dihydro-9,10-ethanoanthracen-12-yl)-propanoate **6**.* A two-necked round-bottom flask containing Pd/C (70 mg, 10%) was wetted with ethanol. After evacuation and charging the flask with hydrogen (H_2, balloon) two times, a solution of unsaturated ester **5** (820 mg, 2.2 mmol) in 15 ml ethanol was added. The mixture was stirred overnight at room temperature under H_2, then filtered through celite with CH_2Cl_2. The solvent was removed in vacuo to obtain the saturated ester **6** (350 mg, 0.93 mmol, 42%) as yellow oil with the following characteristics; **^{1}H-NMR ($CDCl_3$, 400 MHz): $\boldsymbol{\delta}$ =** 1.15–1.2 (m, ^{1}H, H–C11), 1.21–1.30 (m, 4H; ^{1}H –C$'$1, 3H, H–CH_3), 1.47–1.56 (m, ^{1}H, H–C$'$1), 1.87–1.95 (m, ^{1}H, H–C12), 2–2.12 (m, ^{1}H, H–C11), 2.33 (t, J = 12, 2H, H–C$'$2), 4.08 (q, J = 10 Hz, 2H, -O–CH_2–), 4.15 (d, J = 0.4 Hz, ^{1}H, H– C9), 4.26 (t, J = 2 Hz, ^{1}H, H–C10), 7.1–7.20 (m, 3H, ArH), and 7.25–7.35 (m, 3H, ArH) ppm; **HSQC ($CDCl_3$, 100 MHz): $\boldsymbol{\delta}$ =** 14, 30.05 (CH_3), 30.05 (CH_2, C$'$2), 31.15 (CH_2, C$'$1), 34 (CH_2, C11), 38 (C10), 49 (C9), and 60 (CH_2, -O–CH_2–) ppm; **HRMS (ES)** Calcd for $C_{21}H_{20}$ O_2Cl_2Na [M$^+$] 397.0738, Found 397.0735.

3.3. Computational Details

3.3.1. DFT Calculations. Density functional theory (DFT) calculations were performed using Gaussian 09 software [44] for identifying the possible conformers of compound **2**. A hybrid, nonlocal exchange, and correlation functional of Becke-Lee, Parr, and Yang (B3LYP) [45] has been used with the 6-311G (d, p) for DFT calculations. The lowest energy conformers have been obtained by detailed conformation search employing the potential energy scan method.

3.4. Molecular Docking. The interactions of the ligands at the central binding site of LeuT were simulated using Autodock4.2 [46]. The crystal structure of the LeuT protein was downloaded from the Protein Databank [27] and was used as a target by removing all co-crystallized ligands. Discovery studio [25] and Chimera [41] were used to visualize and analyze the docked structures.

4. Conclusion

The synthesis of 1,5-dichloroethanoanthracenes (**2, 3, 5, 6**) has been successfully performed via multistep reactions involving the Diels–Alder and Wittig reactions. In order to identify the structures of the newly synthesized compounds clearly, the structural elucidation techniques, including COSY, HSQC, and HRMS, were extensively employed. The DFT calculations and the experimentally found isomers of aldehyde **2** were in good agreement. From the molecular docking, it can be concluded that all the synthesized

compounds have antidepressant activities and form stable complexes with LeuT by inhibiting the neurotransmitter reuptake at the synapse and hence are good candidates for use as antidepressant drugs. This study will pave way for the researchers to synthesize another 1,5-dichloroethanoanthracene and explore their biological activities as antidepressants, antimalarial agents, and antiproliferative agents.

5. Disclosure

An earlier version of this manuscript has been presented as preprint in Research Square according to the following link: https://www.researchsquare.com/article/rs-515953/v1 [47].

Data Availability

The data used to support the findings of this study are available from the corresponding author upon request.

Conflicts of Interest

The authors declare that they have no conflicts of interest.

Acknowledgments

The authors would like to thank the Deanship of Scientific Research at Umm Al-Qura University for supporting this work by grant code: (22UQU4320141DSR42).

Supplementary Materials

Supplementary Figure. S1. ^{1}H-NMR spectrum of the crude compound 2. Supplementary Figure. S2. IR spectrum of the crude compound 2. Supplementary Figure. S3 (a) ^{1}H-NMR spectrum of the 2a, (b) ^{1}H-NMR spectrum of the 2b, (c) Partial ^{1}H-NMR spectrum of the bridgehead protons (H–C9 and H–C10) of the 2a. Supplementary Figure. S4. ^{13}C NMR spectrum of the 2a. Supplementary Figure. S5 (a)) ^{1}H-NMR spectrum of the 2b, (b) Partial ^{1}H-NMR spectrum of the bridgehead protons (H–C9 and H–C10) of the 2b. Supplementary Figure. S6. ^{13}C NMR spectrum of the 2b. Supplementary Figure S7. IR Spectrum of the compound 1. Supplementary Figure S8. DEPT90 Spectrum of the compound 1. Supplementary Figure S9. DEPT135 Spectrum of the compound 1. Supplementary Figure. S10. HSQC spectrum of the compound 1. Supplementary Figure. S11 (a))^{1}H-NMR spectrum of the compound 5, (b) Partial ^{1}H-NMR of trans isomer 5 at vinylic protons (-CH=CH-), (c) Partial ^{1}H-NMR of trans isomer 5 at bridgehead protons (H–C9, H–C10) and methylene (-O–CH_2–CH_3) as quartet signals of both isomers 5 (cis/trans). Supplementary Figure. S12. IR spectrum of the compound 5. Supplementary Figure. S13. HSQC spectrum of the compound 5. Supplementary Figure. S14. ^{1}H-NMR spectrum of the compound 6. Supplementary Figure. S15. 1H–^{1}H COSY spectrum of the compound 6. Supplementary Figure. S16. HSQC spectrum of the compound 6. Supplementary Figure. S17. HRMS of the compound 6. (*Supplementary Materials*)

References

[1] O. Tosic and J. Mattay, *New Photochromic Dithienylethenes through a Click Chemistry Approach*, Wiley Online Library, Hoboken, USA, 2011.

[2] Q. P. B. Nguyen, J.-N. Kim, and T.-H. Kim, "Investigation of isomerism in anthracene-isothiouronium salts and application of these salts for anion sensing," *Bulletin of the Korean Chemical Society*, vol. 30, pp. 2093–2097, 2009.

[3] J. Langelaar, "Use of time-resolved excited state spectroscopy for selection of laser dyes," *Applied Physics*, vol. 6, no. 1, pp. 61–64, 1975.

[4] C. Schäfer, F. Strübe, S. Bringmann, and J. Mattay, "Photocyclizable resorcin [4] arene dimers," *Photochemical and Photobiological Sciences*, vol. 7, no. 12, pp. 1457–1462, 2008.

[5] J. J. Gassensmith, J. M. Baumes, J. Eberhard, and B. D. Smith, "Cycloaddition to an anthracene-derived macrocyclic receptor with supramolecular control of regioselectivity," *Chemical Communications*, no. 18, pp. 2517–2519, 2009.

[6] S. Bringmann, S. A. Ahmed, R. Hartmann, and J. Mattay, "Synthesis of 1, 5-Substituted Anthracenes by Means of Kumada Coupling and Their Derivatization," *Synthesis*, vol. 2011, pp. 2291–2296, 2011.

[7] I. P. Beletskaya, A. G. Bessmertnykh, A. D. Averin, F. Denat, and R. Guilard, "Palladium-catalysed amination of 1, 8-and 1, 5-dichloroanthracenes and 1, 8-and 1, 5-dichloroanthraquinones," *European Journal of Organic Chemistry*, vol. 2005, no. 2, pp. 281–305, 2005.

[8] E. R. Ranyuk, A. D. Averin, A. K. Buryak et al., "Palladium-catalyzed amination in the synthesis of macrocyclic compounds containing 1, 3-disubstituted adamantane fragments," *Russian Journal of Organic Chemistry*, vol. 45, no. 10, pp. 1555–1566, 2009.

[9] I. P. Beletskaya and A. D. Averin, "Palladium-catalyzed arylation of linear and cyclic polyamines," *Pure and Applied Chemistry*, vol. 76, no. 9, pp. 1605–1619, 2004.

[10] C. F. Chen, Y. X. Ma, and Z. Meng, "Synthesis of substituted iptycenes," *Synlett*, vol. 26, no. 1, pp. 6–30, 2014.

[11] I. Mori, T. Kadosaka, Y. Sakata, and S. Misumi, "Synthesis and spectral properties of chloro-substituted triptycenes," *Bulletin of the Chemical Society of Japan*, vol. 44, no. 6, pp. 1649–1652, 1971.

[12] J.-H. Lamm, J. Glatthor, J.-H. Weddeling et al., "Polyalkynylanthracenes–syntheses, structures and their behaviour towards UV irradiation," *Organic and Biomolecular Chemistry*, vol. 12, no. 37, pp. 7355–7365, 2014.

[13] H. Muhammad, M. Hanif, I. A. Tahiri et al., "Electrochemical behavior of superoxide anion radical towards quinones: a mechanistic approach," *Research on Chemical Intermediates*, vol. 44, no. 10, pp. 6387–6400, 2018.

[14] R. F. Chen, Y. C. Shen, H. S. Huang et al., "Evaluation of the anti-inflammatory and cytotoxic effects of anthraquinones and anthracenes derivatives in human leucocytes," *Journal of Pharmacy and Pharmacology*, vol. 56, no. 7, pp. 915–919, 2010.

[15] R.-F. Chen, C.-L. Chou, M.-R. Wang et al., "Small-molecule anthracene-induced cytotoxicity and induction of apoptosis through generation of reactive oxygen species," *Biological & Pharmaceutical Bulletin*, vol. 27, no. 6, pp. 838–845, 2004.

[16] S. M. Cloonan and D. C. Williams, "The antidepressants maprotiline and fluoxetine induce Type II autophagic cell death in drug-resistant Burkitt's lymphoma," *International Journal of Cancer*, vol. 128, no. 7, pp. 1712–1723, 2011.

[17] Y. McNamara, S. Bright, A. Byrne et al., "Synthesis and antiproliferative action of a novel series of maprotiline

analogs," *European Journal of Medicinal Chemistry*, vol. 71, pp. 333–353, 2014.

[18] M. Wilhelm and P. Schmidt, "Synthesis and properties of 1-aminoalkyl-dibenzo(b, e)bicyclo(2, 2, 2) octadienes," *Helvetica Chimica Acta*, vol. 52, no. 6, pp. 1385–1395, 1969.

[19] N. M. Gray and P. C. Contreras, "Use of bridged tricyclic amine derivatives as anti-ischemic agents," 1991, https://patents.google.com/patent/US5055468A/en.

[20] H. P. Schroeter and Daniel, "Verfahren zur Herstellung von 11-Aminoalkyl-9,10-dihydro-9,10-äthano-anthracenen," 1969, https://www.google.com/search?q=Verfahren+zur+Herstellung+von+11-Aminoalkyl-9%2C10-dihydro-9%2C10-%C3%A4thano-anthracenen&rlz=1C1GCEB_enIN993IN993&oq=Verfahren+zur+Herstellung+von+11-Aminoalkyl-9%2C10-dihydro-9%2C10-%C3%A4thano-anthracenen&aqs=chrome..69i57.339j0j4&sourceid=chrome&ie=UTF-8.

[21] H. Schroter and D. A. Prins, "10-dihydro-11-amino-alkylene-9, 10-ethanoanthracenes," 1969, https://pubchem.ncbi.nlm.nih.gov/compound/601095#section=3D-Conformer.

[22] W. Friebe, U. Tibes, and W. Scheuer, "9, 10-Dihydro-9, 10-ethanoanthracene derivatives as phospholipase inhibitors," 1999, https://patentscope.wipo.int/search/en/detail.jsf?docId=WO1999015493.

[23] K. Nagayasu, "Serotonin transporter: recent progress of in silico ligand prediction methods and structural biology towards structure-guided in silico design of therapeutic agents," *Journal of Pharmacological Sciences*, vol. 148, no. 3, pp. 295–299, 2022.

[24] M. Jarończyk and J. Walory, "Novel molecular targets of antidepressants," *Molecules*, vol. 27, no. 2, p. 533, 2022.

[25] J. A. Coleman and E. Gouaux, "Structural basis for recognition of diverse antidepressants by the human serotonin transporter," *Nature Structural & Molecular Biology*, vol. 25, no. 2, pp. 170–175, 2018.

[26] B. A. Davis, A. Nagarajan, L. R. Forrest, and S. K. Singh, "Mechanism of paroxetine (paxil) inhibition of the serotonin transporter," *Scientific Reports*, vol. 6, pp. 23789–23813, 2016.

[27] Z. Zhou, J. Zhen, N. K. Karpowich et al., "LeuT-desipramine structure reveals how antidepressants block neurotransmitter reuptake," *Science*, vol. 317, no. 5843, pp. 1390–1393, 2007.

[28] A. Robichaud and A. Nait Ajjou, "First example of direct reductive amination of aldehydes with primary and secondary amines catalyzed by water-soluble transition metal catalysts," *Tetrahedron Letters*, vol. 47, no. 22, pp. 3633–3636, 2006.

[29] A. F. Abdel-Magid, K. G. Carson, B. D. Harris, C. A. Maryanoff, and R. D. Shah, "Reductive amination of aldehydes and ketones with sodium triacetoxyborohydride. Studies on direct and indirect reductive amination procedures1," *Journal of Organic Chemistry*, vol. 61, no. 11, pp. 3849–3862, 1996.

[30] B. T. Cho and S. K. Kang, "Direct and indirect reductive amination of aldehydes and ketones with solid acid-activated sodium borohydride under solvent-free conditions," *Tetrahedron*, vol. 61, no. 24, pp. 5725–5734, 2005.

[31] C. Guyon, E. Da Silva, R. Lafon, E. Métay, and M. Lemaire, "Reductive amination using a combination of CaH 2 and noble metal," *RSC Advances*, vol. 5, no. 3, pp. 2292–2298, 2015.

[32] A. Heydari, A. Arefi, and M. Esfandyari, "Direct reductive amination of aldehydes and selective reduction of α, β-unsaturated carbonyl compounds by NaBH 4 in the presence of guanidine hydrochloride in water," *Journal of Molecular Catalysis A: Chemical*, vol. 274, pp. 169–172, 2007.

[33] S. Pisiewicz, T. Stemmler, A. E. Surkus, K. Junge, and M. Beller, "Synthesis of amines by reductive amination of aldehydes and ketones using Co_3O_4/NGr@ C catalyst," *ChemCatChem*, vol. 7, no. 1, pp. 62–64, 2015.

[34] A. I. Khodair, S. E. Kassab, N. A. Kheder, and A. M. Fahim, "Synthesis of novel d-α-galactopyranosyl-l-seryl/l-threonyl-l-alanyl-l-alanine as useful precursors of new glycopeptide antibiotics with computational calculations studies," *Carbohydrate Research*, vol. 514, Article ID 108546, 2022.

[35] A. M. Fahim, H. S. Magar, E. Nasar, F. M. Abdelrazek, and A. Aboelnaga, "Synthesis of Cu-porphyrazines by annulated diazepine rings with electrochemical, conductance activities and computational studies," *Journal of Inorganic and Organometallic Polymers and Materials*, vol. 32, no. 1, pp. 240–266, 2022.

[36] M. Kolář, P. Hobza, and A. K. Bronowska, "Plugging the explicit σ-holes in molecular docking," *Chemical Communications*, vol. 49, no. 10, pp. 981–983, 2013.

[37] A. M. Fahim, A. Mohamed, and M. A. Ibrahim, "Experimental and theoretical studies of some propiolate esters derivatives," *Journal of Molecular Structure*, vol. 1236, Article ID 130281, 2021.

[38] A. M. Fahim, M. A. Shalaby, and M. A. Ibrahim, "Microwave-assisted synthesis of novel 5-aminouracil-based compound with DFT calculations," *Journal of Molecular Structure*, vol. 1194, pp. 211–226, 2019.

[39] B. Kramer, M. Rarey, and T. Lengauer, "Evaluation of the FLEXX incremental construction algorithm for protein–ligand docking," *Proteins: Structure, Function, and Genetics*, vol. 37, no. 2, pp. 228–241, 1999.

[40] D. S. Biovia, *Discovery Studio Modeling Environment*, DassaultSystèmes, 2016.

[41] E. F. Pettersen, T. D. Goddard, C. C. Huang et al., "UCSF Chimera—a visualization system for exploratory research and analysis," *Journal of Computational Chemistry*, vol. 25, no. 13, pp. 1605–1612, 2004.

[42] A. Sanyal, "Chiral anthracenes as Diels-Alder/retro Diels-Alder templates in asymmetric synthesis," 2002, https://www.proquest.com/openview/97bbfcee7423d2a3258220ec70081a5c/1?pq-origsite=gscholar&cbl=18750&diss=y.

[43] U. Karama, M. A. Sultan, A. I. Almansour, and K. E. El-Taher, "Synthesis of chlorinated tetracyclic compounds and testing for their potential antidepressant effect in mice," *Molecules*, vol. 21, no. 1, p. 61, 2016.

[44] M. J. Frisch Gwt, H. B. Schlegel, G. E. Scuseria et al., *Gaussian 09W Reference*, Gaussian, Inc, Wallingford CT, 2009.

[45] A. D. Becke, "Density-functional thermochemistry. III. The role of exact exchange," *The Journal of Chemical Physics*, vol. 98, no. 7, pp. 5648–5652, 1993.

[46] G. M. Morris, R. Huey, W. Lindstrom et al., "AutoDock4 and AutoDockTools4: automated docking with selective receptor flexibility," *Journal of Computational Chemistry*, vol. 30, no. 16, pp. 2785–2791, 2009.

[47] *Mujeeb Sultan RRP EAea 1,5-Dichloroethanoanthracene Derivatives as Antidepressant Maprotiline Analogs: Synthesis and DFT Computational Calculations*, 2021.